# Low pull-in voltage graphene electromechanical switch fabricated with a polymer sacrificial spacer

Jian Sun,[1,a)] Wenzhen Wang,[1] Manoharan Muruganathan,[1] and Hiroshi Mizuta[1,2,b)]
[1]*School of Materials Science, Japan Advanced Institute of Science and Technology, Nomi 923-1211, Japan*
[2]*Nano Research Group, Faculty of Physical Sciences and Engineering, University of Southampton, Highfield, Southampton SO17 1BJ, United Kingdom*

(Received 29 April 2014; accepted 13 July 2014; published online 21 July 2014)

A simple bottom-up procedure using a polymer sacrificial spacer is presented to fabricate graphene electromechanical contact switch devices without using acid etching. Low pull-in voltage of below 2 V is achieved with good consistency on a run-to-run basis, which is compatible with the conventional, complementary metal-oxide-semiconductor circuit requirements. In addition, the formation of carbon-gold bonds at the contact position is proposed as another important mechanism for the irreversible switch—other than the well-known irreversible static friction. © *2014 AIP Publishing LLC*. [http://dx.doi.org/10.1063/1.4891055]

Nanoelectromechanical (NEM) contact switches are attractive components in data storage, high frequency communication, and logic circuits.[1–3] Graphene, as an atomic sheet of graphite, has an ultra-high Young's modulus of ~1 TPa, making it a promising candidate for future NEM applications. The graphene NEM switches showed minimized electrical leakage, sharp switching response, low actuation voltage, and high on/off ratio.[4–7] Despite these potential advantages, graphene has yet to outperform conventional materials because of its low reliability.[4,7] So far, only few reports have shown multiple cycles of switching operation.[5] The common failure is that graphene is stuck on the electrode and not reversible after retracting actuation voltage, which is simply ascribed to an irreversible static friction. However, the details are still unclear. In addition, the switch with suspended graphene achieved using conventional buffered hydrofluoric (BHF) acid etching suffers from some drawbacks.[8] First, BHF attacks titanium, a frequently used adhesive material for Ohmic contact to graphene. Second, as an isotropic process, $SiO_2$ below metal contacts is also removed rapidly. Both of them lead to mechanically unstable structures.[5] Therefore, it is crucial to find a method to produce a suspended graphene device that excludes this aggressive BHF etching step. Recently, several methods have been proposed to realize the suspended graphene on organic polymers without using acid etching.[9,10] However, they all require, at least, two lithography processes. Moreover, the suspended graphene is anchored on a flexible polymer substrate, which may cause damages to the graphene through strain effects.[9]

In this Letter, we report a simple bottom-up procedure to get suspended graphene with a polymer sacrificial spacer, which requires no acid etching and only one lithography process. The two-terminal graphene switches fabricated using the proposed method are characterized. Furthermore, the failure of the irreversible graphene switch is studied to gain a better understanding of the mechanism behind it.

The bottom-up process is illustrated in Fig. 1. First, the 35-nm-thick bottom electrode is defined with a Ti/Au stack on the highly p-doped silicon substrate covered with 300 nm of $SiO_2$ via conventional nanofabrication techniques. Afterwards, a thin polymethyl methacrylate (PMMA) polymer (495 K A4) spacer is spun onto the substrate (Fig. 1(a)), which shows a thickness of ~170 nm after baking. Later, it defines the distance between the suspended graphene and substrate/bottom electrode. Next, graphene is mechanically exfoliated from highly oriented pyrolytic graphite onto the PMMA spacer (Fig. 1(b)). Possible bilayer graphene flakes located on top of the bottom electrode are identified using optical microscopy (left inset of Fig. 2). The bilayer flakes are chosen over monolayer for the higher mechanical strength. Raman spectroscopy (633 nm excitation) is utilized to verify the actual number of layers of the exfoliated graphene (Fig. 2). Four Lorentzian sub-peaks can be fitted to the 2D band (right inset of Fig. 2(b)), showing a clear signature

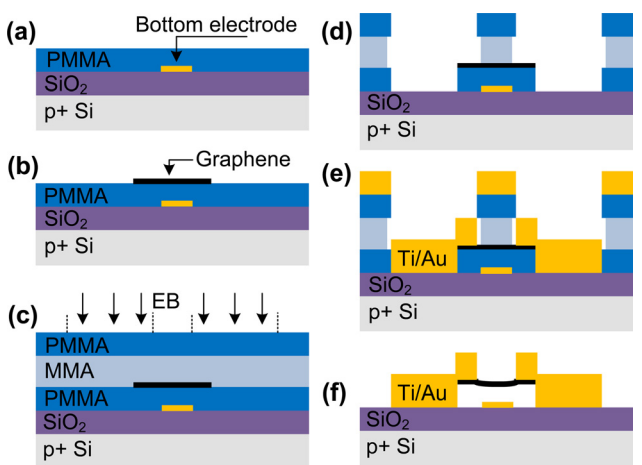


FIG. 1. Schematics of fabrication procedure of graphene switch. (a) PMMA spacer is spin-coated on substrate with pre-defined bottom electrodes. (b) Graphene flakes are mechanically exfoliated onto PMMA spacer. (c) MMA copolymer and PMMA layers are spun in sequence onto substrate, and then EBL is utilized to pattern contacts. (d) Development of the exposed contact areas. PMMA under graphene is protected from development. (e) Metal evaporation. (f) Lift-off and critical point release.

a)sun-jian@jaist.ac.jp
b)mizuta@jaist.ac.jp

 

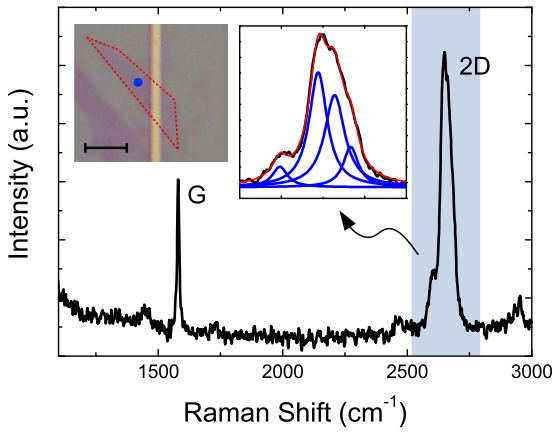


FIG. 2. Raman spectrum of a bilayer graphene on PMMA spacer probed at the blue dot marked in the inset image. Left inset: the microscopic image of graphene flake identified, dot-line shows its edges. The gold strip is the bottom electrode. Scale bar: 5 $\mu$m. Right inset: the Lorentzian peak analysis of 2D band (shadowed). Blue solid curves are the Lorentzian fitted sub-peaks.

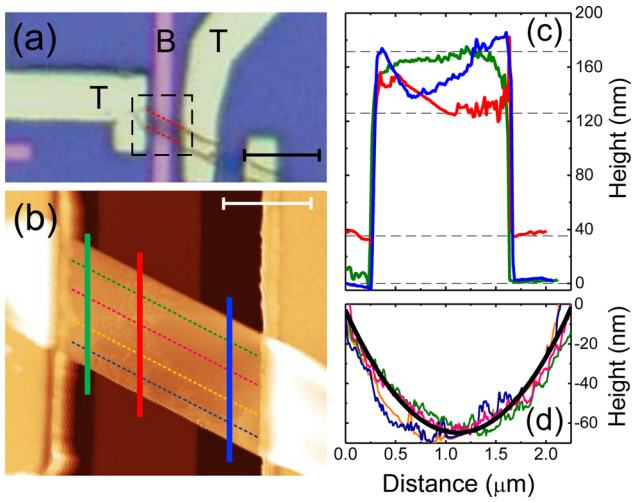


FIG. 3. (a) Microscopic photo of a graphene switch. Red dot-lines indicate the edges of suspended graphene. T and B denote the top and bottom electrode, respectively. Scale bar is 5 $\mu$m. (b) AFM image of the dash-box in (a). Scale bar is 1 $\mu$m. (c) Height profiles measured along the green, red, and blue lines in (b). (d) Longitudinal line scans along suspended graphene with respect to two ends at varied locations (dot-lines in (b)) showing concave buckling. Thick black line is the fitted parabolic curve.

of the bilayer graphene.[11,12] The ratio of the intensity of 2D over the G band, $I_{2D}/I_G$, is found to be ~1.83, which accords with the previously published data.[14] The value is several times larger than that of the graphene on $SiO_2$ substrate, indicating less influence to graphene from PMMA polymer than from $SiO_2$. Furthermore, other valuable information is deduced from the Raman spectrum. D peak is absent, showing a negligible lattice defect in the probed flake. G and 2D bands are found at 1580.3 and ~2650.2 $cm^{-1}$, respectively, without obvious shifting compared with that of the pristine graphene.[11] It manifests that no/weak strain is built in the exfoliated graphene on the PMMA spacer.[13]

After exfoliation, the sample is coated with methylmethacrylate (MMA) 8.5 methacrylic-acid (MAA) EL9 copolymer and PMMA in sequence (Fig. 1(c)). Short baking of 90 s at 180 °C is used for both polymer layers to avoid scrolling and folding in graphene during long thermal treatment.[14] We note that copolymer is first spun rather than PMMA because the solvent of PMMA—anisole—dissolves the PMMA spacer very quickly, hence dislocating graphene during spinning. Top contacts to graphene are defined by using electron beam lithography (Fig. 1(c)). A large electron beam dose is chosen to expose through all polymer layers. After exposure the development process with well-controlled duration opens exposed areas, but leaves the part of the PMMA spacer underneath graphene undeveloped. Top contacts are deposited with 10 nm of Ti and 190 nm of Au in an electron beam evaporator (Fig. 1(e)). The thick metal stack assures the continuity of electrical contacts and the good mechanical stability of the structure. Later, hot N-methyl-2-pyrrolidone (NMP) solvent is used to dissolve all polymers and lift off metal. Finally, the sample is dried using a critical point drier to prevent surface tension induced collapse of suspended graphene (Fig. 1(f)). In principle, this bottom-up method can be applied to any substrates which are insoluble in NMP.

Figure 3(a) displays a bilayer graphene switch fabricated using the aforementioned method. The topographic image is acquired for it using a tapping mode atomic force microscopy (AFM) (Fig. 3(b)). The height profiles in Fig. 3(c) demonstrate that the graphene locates at ~170 nm above the $SiO_2$ substrate near two top electrodes, thereby verifying the graphene's suspension. However, in the center of the graphene, it only exhibits a distance of ~90 nm from the bottom electrode, but not ~135 nm calculated with the 170-nm-thick PMMA spacer and 35-nm-thick bottom electrode for a tabular suspend graphene. This difference is from the concave buckling of the suspended graphene (Fig. 3(d)). It is known as a result of built-in compressive strain and attributed to the negative thermal expansion of graphene in the thermal process.[15] In our fabrication, the 180 °C baking (above the polymer's glass temperature) could lead to relative sliding of graphene with respect to the underlying substrate. When cooled down to room temperature, graphene expands while substrate shrinks, resulting in the contracted carbon bonds, namely, the compressive strain. A similar convex feature was also reported earlier in an acid etching released graphene after thermal treatment.[16] The buckling can be controlled by varying the baking temperature.

We are now to characterize the graphene switch (dimension of graphene: 2.5 $\mu$m × 1 $\mu$m). All measurements are performed at a low pressure of ~0.1 Pa to reduce the impacts from ambience, e.g., the molecular absorption and moisture induced capillary force. First of all, the electrical contact of two top electrodes and leakage current between top and bottom electrodes are examined. Figure 4(a) plots the current-voltage ($I$–$V$) measurements at top-top and top-bottom electrodes, respectively. The linear response between two top electrodes presents Ohmic contact. A low current of ~3 pA is measured between top and bottom electrodes as leakage, which is another evidence of the suspension of graphene.

Figure 4(b) exhibits the performance of the above switch characterized with the two-terminal configuration (inset of Fig. 4(c)). A voltage $V_{tb}$ increased from 0 V is applied between top and bottom electrodes, which electrostatically deflects graphene toward the bottom electrode. At low $V_{tb}$, only leakage current is measured, which is normally referred to as the "switch-off" status. At ~3.5 V, the current abruptly

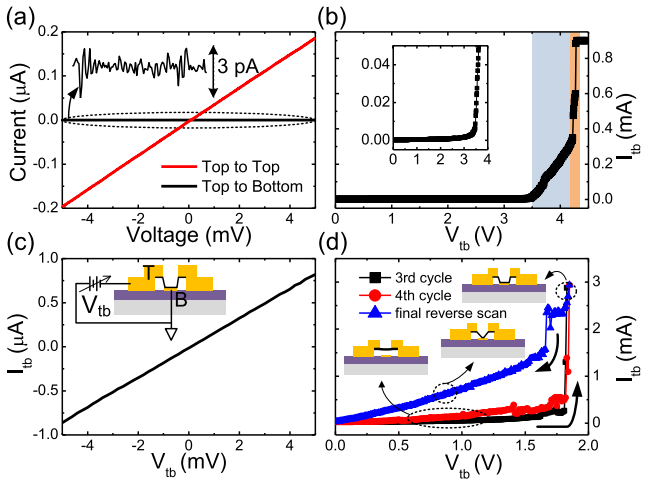


FIG. 4. (a) *I–V* responses at top-top and top-bottom electrodes before switch operation. Inset shows the zoom-in of the leakage current between top and bottom electrodes. $I_{tb}-V_{tb}$ characteristics of the same graphene switch in (a): (b) in operation and (c) after switch's failure; inset of (b) plots the data using a low compliance current. Inset of (c) illustrates the two-terminal configuration. (d) $I-V_{tb}$ characteristics for a different graphene switch at multiple switching cycles. Result of a reverse scan after failure is also provided. Thick arrows show the direction of scan. Insets illustrate different statuses: switch-on, failure, and switch-off (from top).

increases, indicating the physical pull-in of graphene onto the bottom electrode; this is also known as "switch-on." Compared to these using back gates as actuation electrodes,[1] the stronger electrostatic force generated by the local bottom electrode brings about the low pull-in voltage. Interestingly, as voltage continuously increases, we observe a unique transition in current response. The current first increases following a slow slope after pull-in; at ~4.2 V, a transition to a sharper slope suddenly occurs and current dramatically reaches the high compliance current of 0.9 mA. However, this behavior does not emerge if a low compliance is set (inset of Fig. 4(b)). The slow increase of current at the beginning of "switch-on" is probably attributed to the poor electrical contact between graphene and the bottom electrode. A large contact resistance may exist at the interface, as a result of the barrier of adsorbates at the contact interface and small contact area of an incomplete physical pull-in. The Joule heating generated by the current could gradually improve the contact condition. At ~4.2 V, the high current density of $\sim 10^{10}$ A/m$^2$ generates high temperature, which could create carbon-gold (C-Au) bonds by removal of absorbates at the contact interface.[17] Hence, the sudden transition arises. The switch is not reversible after this operation; graphene is stuck on the bottom electrode. Later, a symmetric linear $I_{tb}-V_{tb}$ behavior shows well-established Ohmic contact at the graphene/bottom electrode interface, implying the presence of C-Au bonds (Fig. 4(c)).

A different switch device is also characterized. Here, the applied voltage $V_{tb}$ is immediately retracted once physical pull-in is observed. The Joule heating is limited by shortening the "switch-on" state to prevent the formation of C-Au bonds at the improved contact interface as far as possible. Several cycles of reversible switching are achieved (Fig. 4(d)). Due to a narrower width of graphene (2.5 $\mu$m × 0.5 $\mu$m), a much lower pull-in voltage (~1.85 V) is measured for it compared with the previous one. The consistency of pull-in voltages observed in different cycles is noted, which highlights a good mechanical stability of the structure. A reverse scan of $V_{tb}$ is conducted after the switch's failure. An abrupt drop of current at ~1.65 V, known as pull-out, is still pronounced in the failed switch. However, the current does not promptly reduce to the leakage level, but gradually decreases to zero following a quasi-linear curve, which clearly reveals that contact still partially remains between graphene and the bottom electrode (middle inset of Fig. 4). A large contact resistance read from the small slope of the $I_{tb}-V_{tb}$ curve echoes the little contact area. In this case, we propose that, despite the limited Joule heating, the large potential difference between graphene and the bottom electrode at the moment of pull-in could cause a voltage pulse which is also sufficient to remove absorbates at the first contact position and creates C-Au bonds locally.[17] It interprets the failure as only a small part of graphene remaining in contact, but not as completely collapsed graphene on the bottom electrode. This type of failure could probably be eliminated by coating thin dielectric film on the bottom electrode[5] or using different materials as the bottom electrode.[18]

In summary, we demonstrate the mechanically stable graphene switch fabricated using a simple etching-free method with a polymer sacrificial spacer. A low pull-in voltage of below 2 V is realized. It is compatible with the conventional complementary metal-oxide-semiconductor (CMOS) circuit requirements, showing the possibility of integrating graphene switches into CMOS circuits. A good consistency of the pull-in voltages in multiple cycles highlights the mechanical stability of the switch's structure. The failure mechanism of the irreversible switch is studied. The formation of C-Au bonds at the contact interface is suggested as a possible factor of failure, besides the irreversible static frictions. By limiting them, multiple switching cycles are realized. However, more efforts are still needed to further enhance the reliability of the graphene switch.

This work was supported by Grant-in-Aid for Scientific Research No. 25220904 from Japan Society for the Promotion of Science.

[1]O. Y. Loh and H. D. Espinosa, Nat. Nanotechnol. **7**, 283 (2012).
[2]W. W. Jang, J.-B. Yoon, M.-S. Kim, J.-M. Lee, S.-M. Kim, E.-J. Yoon, K. H. Cho, S.-Y. Lee, I.-H. Choi, D.-W. Kim, and D. Park, Solid-State Electron. **52**, 1578 (2008).
[3]D. A. Czaplewski, G. A. Patrizi, G. M. Kraus, J. R. Wendt, C. D. Nordquist, S. L. Wolfley, M. S. Baker, and M. P. de Boer, J. Micromech. Microeng. **19**, 085003 (2009).
[4]K. M. Milaninia, M. A. Baldo, A. Reina, and J. Kong, Appl. Phys. Lett. **95**, 183105 (2009).
[5]S. M. Kim, E. B. Song, S. Lee, S. Seo, D. H. Seo, Y. Hwang, R. Candler, and K. L. Wang, Appl. Phys. Lett. **99**, 023103 (2011).
[6]M. Nagase, H. Hibino, H. Kageshima, and H. Yamaguchi, Appl. Phys. Express **6**, 055101 (2013).
[7]P. Li, Z. You, G. Haugstad, and T. Cui, Appl. Phys. Lett. **98**, 253105 (2011).
[8]K. I. Bolotin, K. J. Sikes, Z. Jiang, M. Klima, G. Fudenberg, J. Hone, P. Kim, and H. L. Stormer, Solid State Commun. **146**, 351 (2008).
[9]Y. Oshidari, T. Hatakeyama, R. Kometani, S. Warisawa, and S. Ishihara, Appl. Phys. Express **5**, 117201 (2012).
[10]N. Tombros, A. Veligura, J. Junesch, J. Jasper van den Berg, P. J. Zomer, M. Wojtaszek, I. J. Vera Marun, H. T. Jonkman, and B. J. van Wees, J. Appl. Phys. **109**, 093702 (2011).
[11]A. C. Ferrari, J. C. Meyer, V. Scardaci, C. Casiraghi, M. Lazzeri, F. Mauri, S. Piscanec, D. Jiang, K. S. Novoselov, S. Roth, and A. K. Geim, Phys. Rev. Lett. **97**, 187401 (2006).

[12]D. Graf, F. Molitor, K. Ensslin, C. Stampfer, A. Jungen, C. Hierold, and L. Wirtz, Nano Lett. **7**, 238 (2007).
[13]Z. H. Ni, T. Yu, Y. H. Lu, Y. Y. Wang, Y. P. Feng, and Z. X. Shen, ACS Nano **2**, 2301 (2008).
[14]Q. Li, Z. Li, M. Chen, and Y. Fang, Nano Lett. **9**, 2129 (2009).
[15]D. Yoon, Y.-W. Son, and H. Cheong, Nano Lett. **11**, 3227 (2011).
[16]N. Lindahl, D. Midtvedt, J. Svensson, O. A. Nerushev, N. Lindvall, A. Isacsson, and E. E. B. Campbell, Nano Lett. **12**, 3526 (2012).
[17]J. van der Lit, M. P. Boneschanscher, D. Vanmaekelbergh, M. Ijäs, A. Uppstu, M. Ervasti, A. Harju, P. Liljeroth, and I. Swart, Nat. Commun. **4**, 2023 (2013).
[18]O. Loh, X. Wei, J. Sullivan, L. E. Ocola, R. Divan, and H. D. Espinosa, Adv. Mater. **24**, 2463 (2012).